HAL open science

STUDY OF SHAPE EFFECT IN WOUNDED SANDWICH GIANT MAGNETOIMPEDANCE

Christophe Coillot, Joël Moutoussamy, R. Ikhlef, Gérard Chanteur, Francisco Alves

To cite this version:

Christophe Coillot, Joël Moutoussamy, R. Ikhlef, Gérard Chanteur, Francisco Alves. STUDY OF SHAPE EFFECT IN WOUNDED SANDWICH GIANT MAGNETOIMPEDANCE. 2010. hal-00602689

HAL Id: hal-00602689

https://hal.science/hal-00602689v1

Preprint submitted on 23 Jun 2011

HAL is a multi-disciplinary open access archive for the deposit and dissemination of scientific research documents, whether they are published or not. The documents may come from teaching and research institutions in France or abroad, or from public or private research centers.

L'archive ouverte pluridisciplinaire **HAL**, est destinée au dépôt et à la diffusion de documents scientifiques de niveau recherche, publiés ou non, émanant des établissements d'enseignement et de recherche français ou étrangers, des laboratoires publics ou privés.

STUDY OF SHAPE EFFECT IN WOUNDED SANDWICH GIANT MAGNETO-IMPEDANCE

C. Coillot[1], J. Moutoussamy[1], R. Ikhlef[1], G. Chanteur[1] and F. Alves[2]
[1]LPP/CNRS, 10-12 Avenue de l'Europe, Vélizy, FRANCE
[2]LGEP, 11 rue Joliot Curie, Palaiseau, France

Giant Magneto Impedance (GMI) sensors use impedance variation provoked by an external magnetic field. The purpose of this paper is to study the shape effect in wounded GMI sandwich by means of demagnetizing field coefficient computation and his contribution on intrinsic sensitivity magnitude. We first discuss analytic expression of wounded GMI impedance next, and then we derive analytic modelling of intrinsic sensitivity. Finally we compare the theoretical modelling with experimental results taking into account shape effect.

Introduction

Giant Magneto Impedance (GMI) sensors use impedance variation provoked by an external magnetic field. GMI effect has been pointed out in ferromagnetic wires [1], microwires [2], ribbons, sandwiches [3] and transverse or longitudinal wounded sandwiches [4]. Their sensitivity to weak magnetic fields, low mass, and robustness could make them suitable for many applications and especially for space magnetometers application [5]. The invoked physical mechanism implies that magnetic field modifies the dynamic magnetization of the magnetic material and consequently the susceptibility tensor. This last one modifies the skin depth and finally the impedance. Skin effect is usually invoked to describe GMI effect while, in reality, skin effect in sandwich GMI is more complicated than expected due to the lateral skin effect which occurs first in the copper conductor as described in [6]. Simulation results presented on Figure 1, (made on the middle section of Ferro/Co/Ferro sandwich), illustrates lateral skin effect in a copper ribbon at 1MHz (width = 200µm, thickness copper = 20µm). However the skin effect in a ferromagnetic ribbon becomes as expected, when relative permeability is sufficiently high, due to edge effect [7].

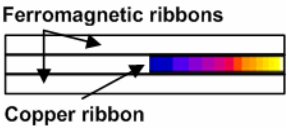

Figure 1. Drawing of GMI sandwich Ferro/Co/Ferro and current density inside its copper ribbon at 1MHz (blue to yellow corresponds to a ratio on the current density magnitude from 1 to 4).

The real GMI sandwich exhibits a poor current conduction between the copper ribbon and the magnetic material ribbons. This experimental fact has led us to neglect the current flowing through the ferromagnetic ribbon and to replace it by coils [8]. In the case of ferromagnetic ribbon, few authors have noticed the role of demagnetizing field in the improvement of GMI effect [9]. In the following we focus on theoretical and experimental results taking into account shape effect

Impedance modelling of wounded GMI sandwich

We consider the wounded sandwich GMIs described on Figure 2. In that case, the existence of the skin effect inside the GMI becomes obvious as the wires are now insulated. In order to focus on shape effect our study will concern transverse wounded GMI (Figure 2.a) using a single ferromagnetic ribbon. Moreover by neglecting losses inside the magnetic material we easily compute, for transverse wounded GMI represented on Figure 2.a), the impedance at null field. This impedance, called Zgmi, is given by equation (1).

$$Z_{gmi} = R(\omega) + jL_0\mu_{app}(\omega)\omega = R(\omega) + j\frac{N^2 \cdot \mu_0 \cdot S}{l_{ribbon}}\mu_{app}(H,\omega)\cdot\omega \quad (1)$$

$$\mu_{app} = \frac{\mu_r}{1 + N_x \cdot (\mu_r - 1)} \quad (2)$$

Where, R is the resistance of the N turns winding, L_0 is the inductance of the air-coil, μ_0 is the air permeability, S is the cross-section area of the ribbon, l_{ribbon} is the length of the ribbon, μ_{app} is the apparent permeability in x direction expressed by (5), μ_{ri} is the initial relative permeability of the material and N_x the demagnetizing factor coefficient in x direction (similarly N_y is the demagnetizing factor in y direction). To compute the demagnetizing factor, the ribbon is approximated by an ellipsoid and the formulas given in [10], for the case of very flat ellipsoid, are used.

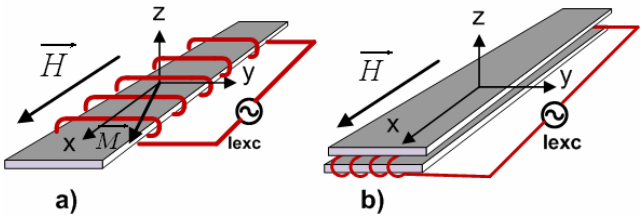

Figure 2. Transverse (a) and Longitudinal (b) wounded GMI.

Intrinsic sensitivity and bias field parameters

We now consider the behaviour of wounded GMI sandwich, flown by an excitation current (I_{EXC}), inside a homogeneous magnetic field. We focus on the main relevant parameters to characterize GMI performances which are: bias field (should be lowest as possible to reduce current consumption) and intrinsic sensitivity (defined as the slope of Z(H)). When an external magnetic field (H) is applied to the transverse wounded GMI, the *Zgmi(H)* characteristic behaves as represented on Figure 3.a). We notice that above a magnetic field called H_{ani} the impedance starts to vary with magnetic field. This field can be interpreted as an effective anisotropic magnetic field. Next the figure 3.b) represents the slope of Z(H) (called intrinsic sensitivity S_I as defined by eq. (3)). This intrinsic sensitivity is fully relevant to characterize the ability of GMI to measure a weak magnetic field [8].

$$S_I = \frac{\partial Z}{\partial H} \tag{3}$$

We can notice from Figure 3.b), that an optimum bias field (H_{BIAS}) corresponding to the maximum of S_I occurs.

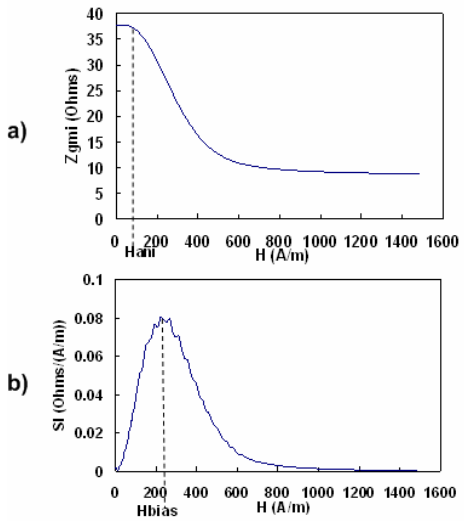

Figure 3: a) GMI sandwich impedance and b)GMI sandwich intrinsic sensitivity(V/µT) under magnetic field.

Let us focus on the computation of the anisotropic field. We first express the magnetostatic energy of the ribbon completed by the demagnetizing field energy and magnetocrystalline anisotropy energy. We assume magnetocrystalline anisotropy in the x direction and magnetization in x,y plane, that leads to eq. (4).

$$E = -\mu_0 \vec{H}\vec{M} - \frac{1}{2}\mu_0 \vec{H_d}\vec{M} + K_u \sin^2\varphi \tag{4}$$

In this later expression, φ represents the angle between magnetization ($\vec{M}$) and easy magnetization axis (x axis), $\vec{H_d}$ detailed in equation (5) represents the demagnetizing magnetic field.

$$\vec{H_d} = -\begin{bmatrix} N_x & 0 \\ 0 & N_y \end{bmatrix} \times \begin{bmatrix} M\cos\varphi \\ M\sin\varphi \end{bmatrix} \tag{5}$$

Next, by minimizing magnetostatic energy (from eq. (4)) we obtain the values of magnetic field for which magnetization rotates:

$$H > H_{ani} = \frac{(N_y - N_x)M^2 + 2K_u/\mu_0}{M} \tag{6}$$

This latest expression suggests that both magnetocrystalline anisotropy and demagnetizing factor (i.e. the shape effect) dictates the magnetization behavior and value of the anisotropic effective magnetic field. Finally the demagnetizing factor will both affects the transverse permeability of the material (μ_t) and its longitudinal permeability (μ_l), which is involved in the longitudinal GMI effect.

Shape effect in wounded GMI

We now consider GMI impedance (eq (4)) by taking into account his dependence to magnetic field. It seems relevant to use magnetic field internal to the ribbon (Hgmi) and to divide the intrinsic sensitivity in the following way:

$$S_I = \frac{\partial Z}{\partial H_{gmi}} \times \frac{\partial H_{gmi}}{\partial H} \tag{7}$$

From classical magnetostatic equations [8], one can link the external magnetic field (H) to the internal magnetic field (H_{gmi}), using eq. (8).

$$H_{gmi} = \frac{H}{1 + N_x(\mu_r(H_{gmi}) - 1)} \tag{8}$$

Then, we deduce:

$$\frac{\partial H_{gmi}}{\partial H} = \frac{1}{\left(1 + N_x \cdot \mu_r(H_{gmi})\right) + H_{gmi} \cdot N_x \cdot (\partial\mu_r(H_{gmi})/\partial H_{gmi})} \tag{9}$$

Finally, we derivate (1) accordingly to Hgmi and substitute its result inside eq. (7) to obtain this latest expression:

$$\left|\frac{\partial Z}{\partial H}\right| = \frac{L_0\omega \times (\partial\mu_r/\partial H_{gmi})}{(1 + N_x \cdot \mu_r)^2 \cdot \left[(1 + N_x \cdot \mu_r) + H_{gmi} \cdot N_x \cdot (\partial\mu_r/\partial H_{gmi})\right]} \tag{10}$$

The intrinsic sensitivity, expressed by eq. (10), shows clearly the dependence with magnetic material behaviour $\partial\mu_r/\partial H_{gmi}$ around a magnetic bias point $\mu_r(H_{gmi})$, but also, the role of the demagnetizing field coefficient in the direction of the measurement (N_x) [9]. This dependence suggests strongly that demagnetizing factor, and thus the shape effect, is of great importance in the value of the intrinsic sensitivity.

Experimental results and comparisons with model

Measurements of intrinsic sensitivity have been performed on longitudinal wounded GMI. The coil was supply at low frequency (few kHz). Ribbons, used to build the sensors, are made of commercial ultraperm [11] with various lengths (20mm up to 50mm) and various thicknesses (from 50µm to 350µm). Intrinsic sensitivities (S_I) for ribbons of different lengths are plotted on Figure 4.a. These curves show an important increase of maximal S_I when length increases, while the optimal bias field decreases (corresponding to maximum of SI). The decrease of bias field is synonymous of lower power to bias the magnetic material. Similarly, Figure 4.b shows an increase of S_I when thickness of the ribbon decreases while the bias field also decreases.

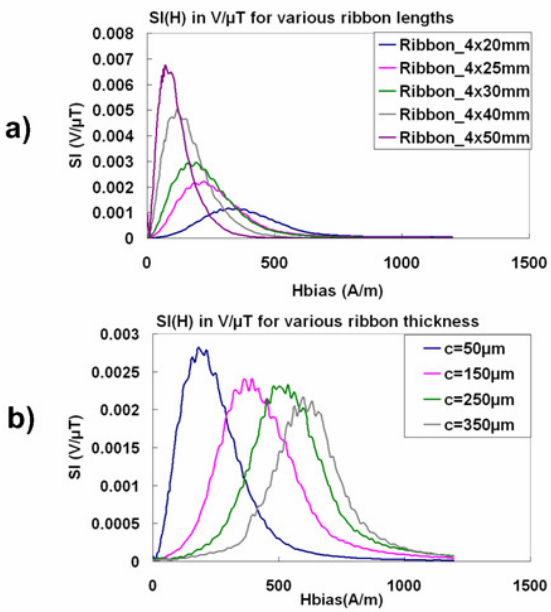

Figure 4. Measurement of intrinsic sensitivity of 4mm width GMI ribbon for various length (20mm to 100mm) and 30mm ribbon length for various thickness (50µm to 350µm).

These experimental results confirm the important role of shape effect. A small demagnetizing field, in the direction of measurement, will imply a great S_I while the bias field required will be reduced.

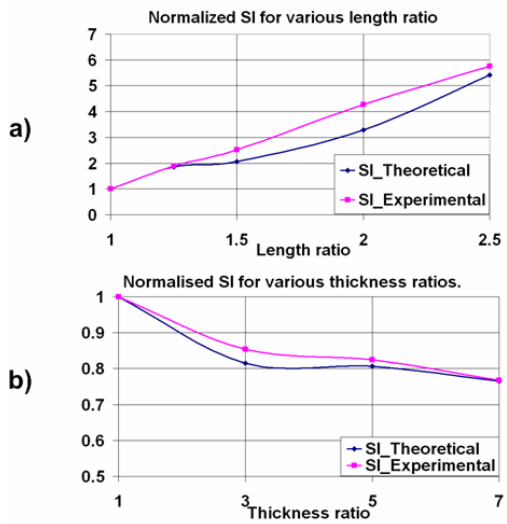

Figure 5.Comparison of measured and computed intrinsic sensitivity at optimal bias field for various length ratio (a) and thickness ratio (b).

Let us try to compare the experimental results to the modelling. In order to make the comparison, it is necessary to extract data from experimental conditions. Value of the experimental optimal bias field is used to compute the operating point of the magnetic material (in terms of Hgmi and µr(Hgmi)). The latter (µr(Hgmi)) is deduced from the real B(H) curve of the material from [9]. Next, Equation (10) is applied to compute intrinsic sensitivity at the optimal bias field. The normalized comparison between experimental results and modelling is presented on Figure 5, both for length ratio effect (Fig. 5.a) and thickness ratio effect (Fig 5.b). Instead of small discrepancies, due to the operating point determination extracted from datasheet, we can notice that theoretical modelling combined to material characteristics give a good estimate of the tendency of S_I.

Conclusion

The experimental results confirm that reduction of the demagnetizing field factor in the direction of the measurement of the ferromagnetic part (ribbon as well as wire) is fully relevant, for a given magnetic material, to increase intrinsic sensitivity of GMI. This effect is sometime evoked [8] but never, at our best knowledge, computed.

Acknowledgements.

The authors would like to thank CNES (Space French Agency) who has funded this work.

REFERENCES:

[1] E.P. Harrison, G.L Turney, H. Rowe, H. Gollop, “The electrical properties of High permeability Wires Carrying Alternating Current”, Proc. Royal. Soc, Vol 157, 1936

[2] Panina L.V., Mohri, K., “Magneto-impedance effect in amorphous wires”, Applied Physics Letter 65, pp. 1189-1191, 1994.

[3] K.Hika et al., “Magneto-Impedance in Sandwich Film for Magnetic Sensor Heads”, IEEE Trans. Magn, Vol. 32, pp. 4594-4596, 1996.

[4] J. Moutoussamy, C. Coillot, F. Alvès, G. Chanteur, “Longitudinal and transverse coiled giant magnetoimpedance transducers: principle, modelling and performances”, Transducer’09 (Colorado-USA), June 2009.

[5] W. Magnes et al, “A sigma-delta fluxgate magnetometer for space applications », Meas. Sci. Technology, n°14, pp 1003-1012, June 2003.

[6] Belevitch V., “The lateral skin effect in a flat conductor”, Philips tech Rev., n° 32, pp 221-231, 1971.

[7] Garcia-Arribas A., Barandiaran J.M., de Cos D., « Finite element method calculations of GMI in thin films and sandwiched structures: size and edge effects », Journal of Magnetism and Magnetic Materials, Volume 320, pp. e4-e7, 2008

[8] J. Moutoussamy, C. Coillot, F. Alvès, G. Chanteur, “Feasibility of a giant magneto-impedance sandwich magnetometer for space applications”, IEEE Sensors Conference (Atlanta-USA), pp 1013-1016, Oct. 2007.

[9] L.A.P. Goncalves, J.M. Soares, F.L.A Machado, W.M. de Azevedo, “GMI effect in the low magnetostrictive CoFeSiB allos”, Physica B 384 (2006), pp 152 154.

[10] J.A. Osborn, “Demagnetizing factors of the general ellipsoids”, Phys. Review, Vol 67, pp. 351-357, 1945.

[11] Vacuumschmelze GMBH & Co Kg, « Soft Magnetic Materials and Semi-Finished Products », Edition 2002.